Deep-Sea Research II 101 (2014) 120–128

Contents lists available at ScienceDirect

Deep-Sea Research II

journal homepage: www.elsevier.com/locate/dsr2

Phytoplankton patchiness during spring intermonsoon in western coast of South China Sea

Jiu-Juan Wang [a,b], Dan Ling Tang [a,b,*]

[a] Research Center for Remote Sensing of Marine Ecology & Environment, State Key Laboratory of Tropical Oceanography, South China Sea Institute of Oceanology, Chinese Academy of Sciences, Guangzhou 510301, China
[b] University of Chinese Academy of Sciences, Beijing 100049, China

ARTICLE INFO

Available online 21 September 2013

Keywords:
Wind-stress curl
Phytoplankton patchiness
Upwelling
Intermonsoon
South China Sea

ABSTRACT

Jet-like phytoplankton blooms usually occur off the southwestern coast of the South China Sea (SCS) caused by strong winds during summer monsoons. However a jet-like phytoplankton patch was observed in the western SCS in the spring intermonsoon of 2010 in both field and remote sensing data. The present study investigated the biological processes associated with this spring phytoplankton patchiness. The data showed that chlorophyll *a* concentrations increased in the surface water, extending out to the SCS, and the depth of the subsurface chlorophyll maximum uplifted from 75 m to 50 m depth; low dissolved oxygen, low pH and nutrient enrichment (nitrate+nitrite and soluble reactive phosphate) were observed in the subsurface water (50 to ~200 m depth). Data analysis showed that variations in chlorophyll *a*, nutrients and temperature in the water column were related to wind-stress curl: the spatial distribution pattern and vertical structure of the phytoplankton patchiness were controlled by vertical flux of nutrients caused by curl-driven upwelling through Ekman pumping. There was a high correlation between chlorophyll *a* concentration and wind-stress curl where the influence of nutrient influx from the coast was limited. This study shows the importance of wind-stress curl in providing nutrients to support phytoplankton growth during the spring intermonsoon along the western coast of SCS. It may help to better understand the role of wind in marine biological processes.

1. Introduction

Over most of the South China Sea (SCS), the phytoplankton biomass is low and controlled by monsoons (Ning et al., 2004). The climate of the SCS is part of the Asian monsoon system, where northeast monsoons occur in winter and southwest monsoons occur in summer (Liu et al., 2002). In the southwestern coastal region of the SCS, phytoplankton blooms, including harmful algal blooms (HABs), frequently occur in summer when southwest monsoons are parallel to the Vietnamese coast (Tang et al., 2004a, 2004b). Long-term observations indicate that these phytoplankton blooms are consistent phenomena appearing almost every summer (Tang et al., 2004a, 2005). In the upper layer of the open ocean, the supply of new nutrient is one of the primary factors controlling the growth of phytoplankton (McGillicuddy et al., 2003), and physical processes control nutrient flux into the euphotic zone and hence play a profound role in the phytoplankton growth and their temporal and spatial distribution (Cloern, 1996). Monsoon-induced coastal upwelling is one of the most important processes in the physical oceanography of the SCS and can deliver ample new nutrients to sustain the phytoplankton growth (Tang et al., 2002; Botsford et al., 2006). The persistent alongshore southwest monsoon forces Ekman transport and the resultant coastal upwelling delivers nutrients to surface waters and sustains high phytoplankton biomass (Tang et al., 2004a; Dippner et al., 2007). Xie et al. (2003) found that an anticyclonic eddy develops from the Vietnam coast to the open SCS in July and August, advecting coastal water in the form of coastal filaments. The distribution of coastal filament displays large interannual variability associated with changes in the SCS ocean circulation. Phytoplankton patchiness is associated with the coastal filament during this period. The resultant anticyclonic eddy may have impacts on the spatial distribution of phytoplankton biomass during the summer monsoon season (Tang et al., 2004a). The summer blooms of the haptophyte genus *Phaeocystis* are often observed in the coastal upwelling region off the coastal Vietnam during southwest monsoon (Tang et al., 2004b; Hai et al., 2010). The phytoplankton blooms subsequently disappear when the southwest monsoon ends.

* Corresponding author at: Research Center for Remote Sensing of Marine Ecology & Environment, State Key Laboratory of Tropical Oceanography, South China Sea Institute of Oceanology, Chinese Academy of Sciences, Guangzhou 510301, China. Tel.: +86 20 8902 3203.
E-mail address: lingzistdl@126.com (D.L. Tang).
URL: http://lingzis.51.net/ (D.L. Tang).

0967-0645/$ - see front matter © 2013 Elsevier Ltd. All rights reserved.
http://dx.doi.org/10.1016/j.dsr2.2013.09.020

In this region the intermonsoon is a transition period between summer and winter monsoons; the spring intermonsoon is from March to June (Voss et al., 2006). During the intermonsoon, the wind direction is variable and patterns tend to be very chaotic (Corrigan et al., 2006). Consequently wind stress during intermonsoon seasons does not usually induce persistent coastal upwelling. In the absence of southwesterly winds, the anticyclonic ocean circulation is weakest in the spring intermonsoon in the SCS (Hwang and Chen, 2000). Oligotrophic conditions prevail during most of the spring intermonsoon period. Based on field measurements, Voss et al. (2006) found that nitrogen fixation rates and other hydro-chemical variables during the spring intermonsoon of 2004 were 10 times lower than in the summer monsoon. In May, 2003, a phytoplankton bloom was reported during this oligotrophic period (Lin et al., 2010). Many studies have investigated primary productivity and the coupling of biological–physical processes in monsoon seasons in the SCS, but little attention has been focused on the dynamic features of phytoplankton during intermonsoon.

In the present work, a jet-like phytoplankton patchiness was observed in the western coastal area of the SCS during the spring intermonsoon in 2010. A key question was can this phytoplankton patchiness occur without alongshore winds during intermonsoon season? Can the chaotic winds during this period contribute to the spring phytoplankton patchiness? We combined in situ observations together with analysis of remote sensing data to elucidate the phytoplankton patchiness and related dynamic processes. The objective of this work was to identify how winds during spring intermonsoon regulate the phytoplankton patchiness on spatial distribution and vertical structure in the upper ocean.

2. Data and methods

2.1. Study area and in situ observations

The study area comprises the eastern Vietnamese coastal water and adjacent western SCS (Fig. 1A and B). In situ observations were made between May 7 and 16, 2010 at 15 sampling stations (Fig. 1B) along the ship's track. The stations were more than 1000 m in depth. Seawater temperature profiles were obtained at each station using a Sea-Bird SBE9 Conductivity–Temperature–Depth (CTD). Seawater samples were collected with Niskin bottles triggered at various depths (surface, 25 m, 50 m, 75 m, 100 m, 150 m, and 200 m). Seawater samples for dissolved oxygen analysis were carefully taken in calibrated dry glass bottles from the Niskin bottles. Dissolved oxygen concentrations were measured using automated precision Winkler titration using a Metrohm 716 DMS Titrino (Oudot et al., 1988; Pomeroy et al., 1994). The seawater pH were measured immediately after samplig using a Mettler Toledo pH meter. The in situ pH values were corrected for depth and pressure. Seawater samples for chlorophyll *a* concentration analysis were filtered onto 25 mm Whatman glass fiber filters (GF/F) and then quickly frozen in dark until analysis in laboratory. Chlorophyll *a* was extracted in ice-cold 90% v/v acetone and measured using a Turner Designs TD-700 fluorometer with 436 nm excitation filter and 680 nm emission filter. Concentrations of nitrate + nitrite (NO_x) and soluble reactive phosphate (SRP) were analyzed on a flow injection analyzer (FIA Lachat QC8500, Lachat Instruments, USA) using the standard pink azo dye and phosphorus molybdenum blue method, respectively (Strickland and Parsons, 1972).

2.2. Remote sensing data and analysis

Remote sensing data of sea surface chlorophyll *a* concentration, the normalized water-leaving radiance at wave-length 443 nm (*nLw* (443)) and 555 nm (*nLw* (555)), with 1 km × 1 km spatial resolution, were derived from MODerate resolution Imaging Spectroradiometer (MODIS) onboard Aqua, launched in 1999. A strong absorption of phytoplankton is at *nLw* (443) (Shi and Wang, 2007). The *nLw* (555) denotes suspended sediment and hence the influence of coastal water (Zheng and Tang, 2007). We compared *nLw* (443) and *nLw* (555) with sea surface chlorophyll *a* concentration to determine the influence of coastal water on the formation of the phytoplankton bloom. Raw satellite data were obtained from the NASA OceanColor Website. To investigate the temporal variation, we composited 8-day averaged chlorophyll *a* images.

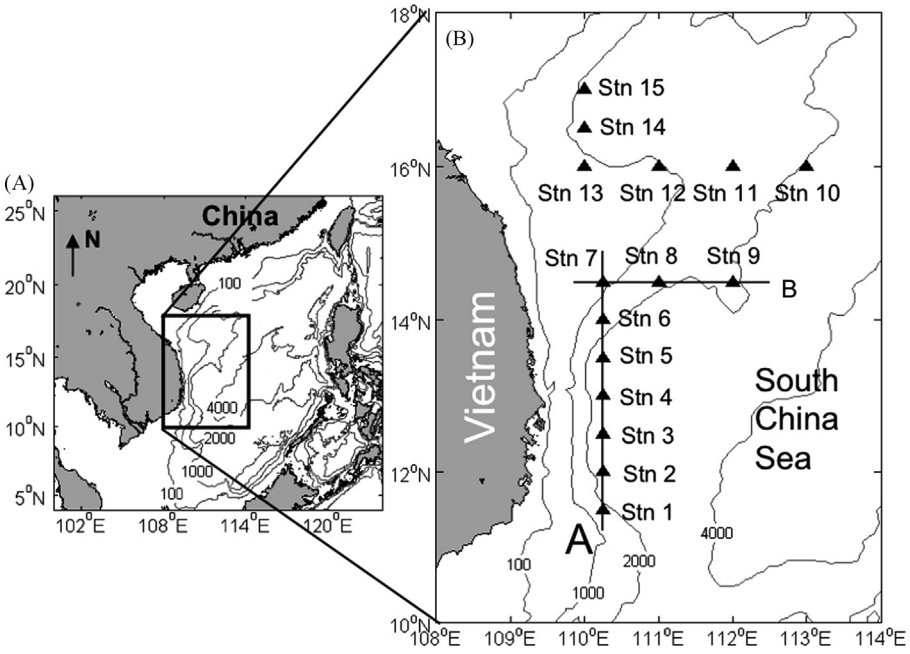

Fig. 1. (A) The geographic location and bathymetry of the study region in the western South China Sea. (B) Locations of sampling stations and transects A and B in the western South China Sea between May 7 and May 16, 2010.

The Advanced SCATterometer (ASCAT), onboard the EUMETSAT METOP satellite (launched 19 October 2006) was used to determine 10 m neutral stability wind. ASCAT wind vectors were obtained from the NOAA Environmental Research Division's Data Access Program. To investigate the influence of wind forcing on phytoplankton, we calculated wind-stress curl, Ekman pumping velocity (EPV) and Ekman mass transport (EMT) based on ASCAT wind vectors:

$$curl = \partial\tau_y/\partial x - \partial\tau_x/\partial y; \quad EPV = -curl/\rho_w f; \quad EMT = \tau/\rho_w f.$$

where ρ_a is the density of air (1.25 kg m^{-3}), ρ_w is the density of seawater (1.025×10^3 kg m^{-3}), C_d is the drag coefficient (2.6×10^{-3}), U_{10} is the wind speed 10 m above sea level derived from ASCAT wind vectors, τ is the wind stress ($\tau = \rho_a C_d U_{10}^2$), θ is the latitude (in radians), and f is the Coriolis parameter (Stewart, 2008). To compare the changing trend of wind with surveyed data, we selected wind data with the same locations of the sampling station from 8-day averaged ASCAT wind data during the same period. All the calculations were done using Matlab R2008a.

8-day averaged MODIS chlorophyll *a* and ASCAT wind from May 30 to June 6, 2010 were analyzed using the Pearson Correlation analysis (SPSS 16.0).

3. Results

3.1. Field investigation of the spring phytoplankton bloom

Sea surface biological and chemical characteristics at the fifteen sampling stations off the eastern coast of Vietnam are shown in Fig. 2. The average surface chlorophyll *a* was 0.07 mg m^{-3} across all sampling stations (Stations 1–15). However, the chlorophyll *a* at Station 7 was 0.15 mg m^{-3}, twice the average value (Fig. 2A). The average NO_x and SRP were 2.71 μM and 0.43 μM, respectively, and the average dissolved oxygen was 6.51 mg m^{-3}. The lowest observed NO_x (1.76 μM) (Fig. 2B) and SRP (0.34 μM) (Fig. 2C) and the highest dissolved oxygen (7.03 mg m^{-3}) (Fig. 2D), were all observed at Station 7 corresponding to the highest chlorophyll *a* level.

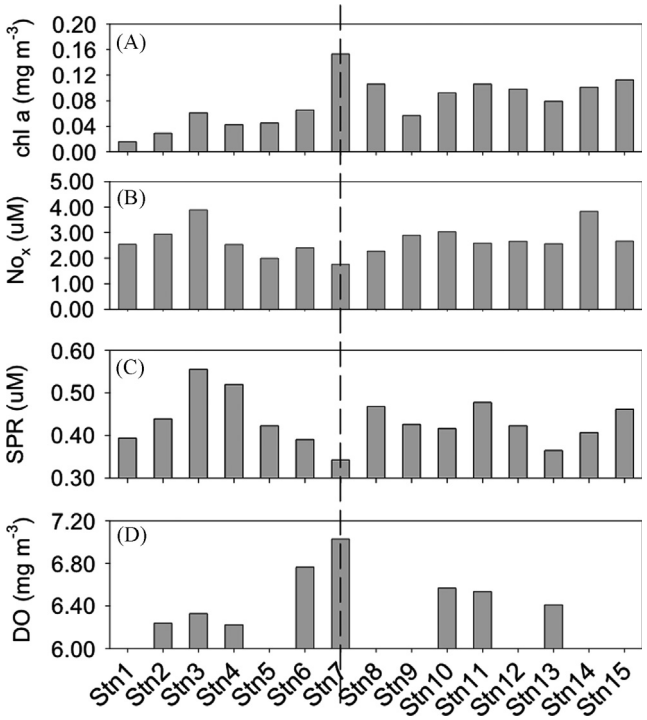

Fig. 2. Surface concentrations of (A) chlorophyll *a*, (B) nitrate+nitrite (NO_x), (C) soluble reactive phosphate (SRP) and (D) dissolved oxygen (DO) at the sampling stations off the eastern coast of Vietnam during the spring intermonsoon, 2010. Sampling station locations are shown in Fig. 1B.

A comparison of the profiles of nutrients (NO_x and SRP), dissolved oxygen and pH at Stations 1, 7, and 15 is shown in Fig. 3. Between the depths of 50 m and 150 m, the average concentrations of NO_x were 7.84 μM (Station 7), 6.41 μM (Station 1) and 6.14 μM (Station 15). The average concentration of SRP at Station 7 (> 0.57 μM) was slightly higher than those at Station 1 (0.55 μM) and Station 15 (0.49 μM), respectively. The average dissolved oxygen concentration (< 5.48 mg m^{-3}) and pH (ca. 7.98) were relatively low at Station 7.

Fig. 4 shows the variations in subsurface chlorophyll maximum and vertical structure of chlorophyll *a* in the upper 200 m. Chlorophyll *a* concentrations increased with depth, reaching highest values at a depth of 50–75 m (Fig. 4A). The highest chlorophyll *a* concentration was ca. 0.4 mg m^{-3} among all stations except for Station 7, where the subsurface chlorophyll maximum concentration increased to more than 1.4 mg m^{-3} and was uplifted to a depth of 50 m (Fig. 4A). The vertical structure of chlorophyll *a* along transects "A" and "B" (Fig. 1A) showed that around Station 7 higher chlorophyll *a* concentrations were present in the euphotic zone and the isopleths of chlorophyll *a* were elevated (Fig. 4B).

The water column average chlorophyll *a* over the upper 200 m ranged from 0.12 mg m^{-3} to 0.35 mg m^{-3}. The enhanced chlorophyll *a* at Station 7 (Fig. 5A) co-incided with the lowest sea water temperature (20.2 °C; Fig. 5B), the highest NO_x (9.09 μM; Fig. 5C) and highest SRP (0.60 μM; Fig. 5D). Moreover, the variations in wind-stress curl (1.41×10^{-6} N m^{-3} to 2.71×10^{-6} N m^{-3}) and wind speed (3.71 m s^{-1} and 7.78 m s^{-1}) during the sampling period were comparable with those in water column average chlorophyll *a* (Fig. 5A).

3.2. Spatial distributions of chlorophyll a concentrations and wind

The 8-day averaged MODIS chlorophyll *a* concentrations revealed variations in the phytoplankton biomass off the eastern coast of Vietnam during the spring intermonsoon, 2010 (Fig. 6A). In late April (4/19–4/26), chlorophyll *a* concentrations were generally low (< 0.1 mg m^{-3}) in the western SCS. In early May (4/27–5/4), the phytoplankton biomass patchiness was initially formed and the high chlorophyll *a* concentrations appeared slightly offshore extending to 110°E along 14°N. In the middle May (5/5–5/13), the phytoplankton bloom intensified. Significant offshore phytoplankton biomass patchiness was exhibited as a jet-like shape from the eastern Vietnamese coast to the southwestern SCS in late May (5/30–6/6).

Wind speed was generally low (ca. 5.6 m s^{-1}) and wind direction followed an unpredictable pattern (Fig. 6B) during the spring intermonsoon. In late April, wind directions were generally from east to northwest, and switched to northeast in the middle of May. In late May, wind blew from the southwest to northeast with an increasing speed. The contours in Fig. 6B show the spatial variations of wind-stress curl calculated from ASCAT wind vectors. In late April, the wind-stress curl was largely negative (less than -6.7×10^{-7} N m^{-3}). In early and middle May, the distribution patterns of positive wind-stress curl were similar to that of chlorophyll *a* in the same period. This phenomenon was manifested in late May. In this period, the pattern of positive wind-stress curl took the form of a jet off the east coast of Vietnam, similar to the pattern in phytoplankton biomass patchiness. Ekman pumping velocity (Fig. 6C) and Ekman mass transport (Fig. 6D) are two important effects of winds. In late April, the Ekman pumping velocity was largely positive, and the Ekman mass transport was from southwest to northeast. In early and middle-May, the negative Ekman pumping velocity was evident along the Vietnamese coast extending to the SCS and, in the same period, the Ekman mass transport was slight with changing

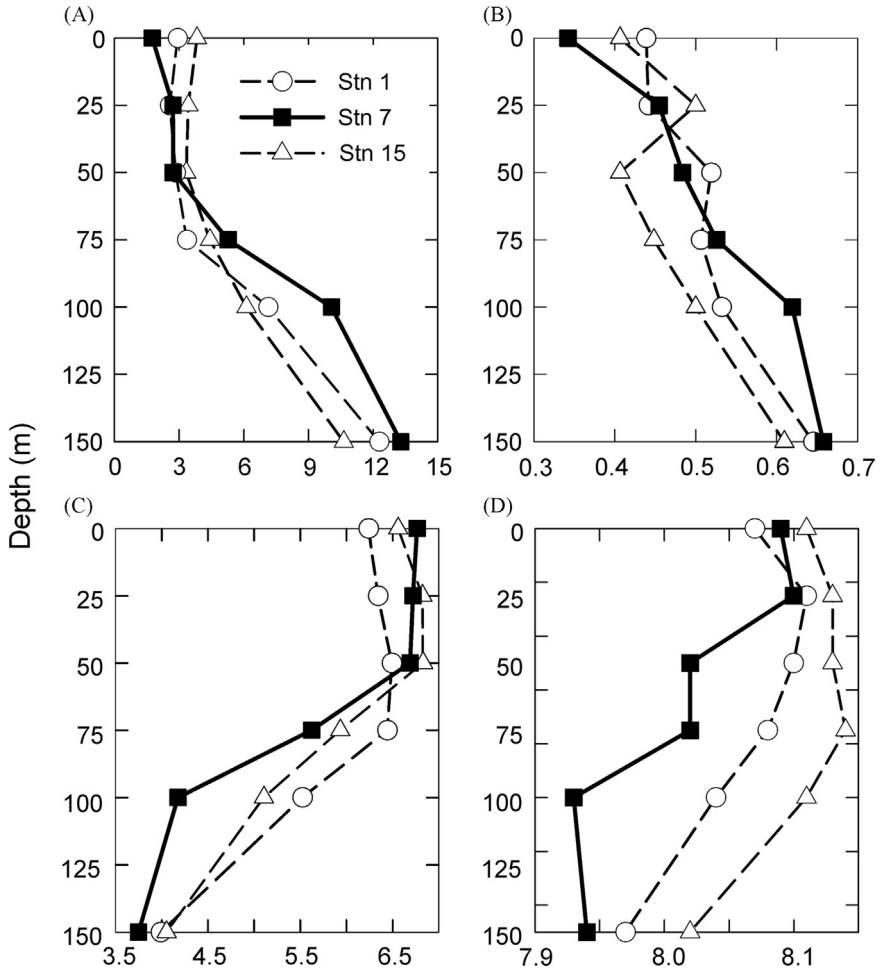

Fig. 3. Vertical profiles of (A) nitrate+nitrite (NO_x) (μM), (B) soluble reactive phosphate (SRP) (μM), (C) dissolved oxygen (DO) (mg L^{-1}) and (D) pH at Station 1 (open circles), Station 7 (filled squares) and Station 15 (open triangles). For station locations see Fig. 1B.

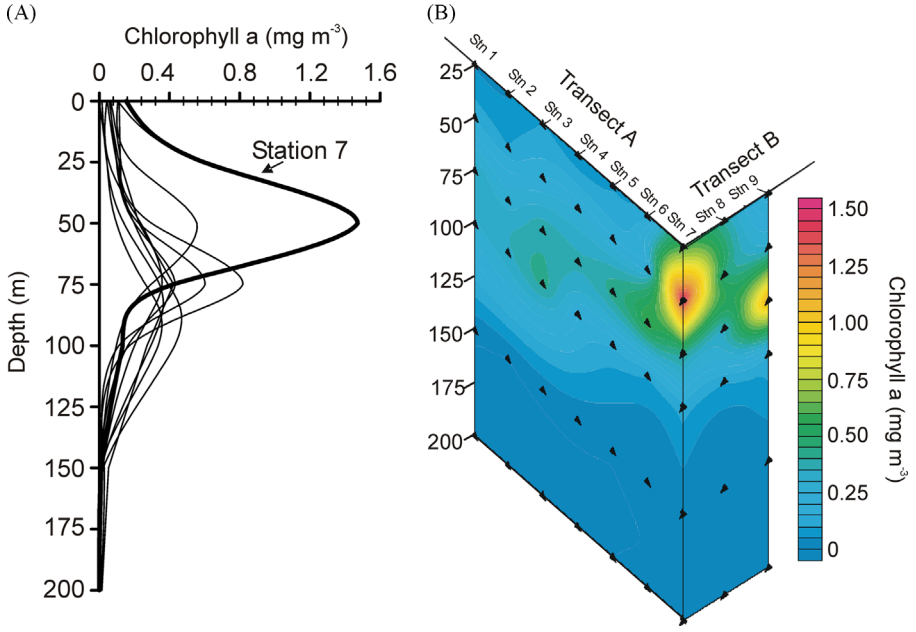

Fig. 4. (A) Representative vertical profiles of chlorophyll *a* concentration across the sampling stations and (B) the vertical structure of Chl *a* concentrations along transects A and B (see Fig. 1B).

directions. The high Ekman pumping velocity and Ekman mass transport were observed in late May with different patterns. The pattern of negative high Ekman pumping velocity was similar to a plume off the Vietnam coast in the nearby SCS; the pattern of high Ekman mass transport was located in the center of southwest SCS with the direction from northwest to southeast.

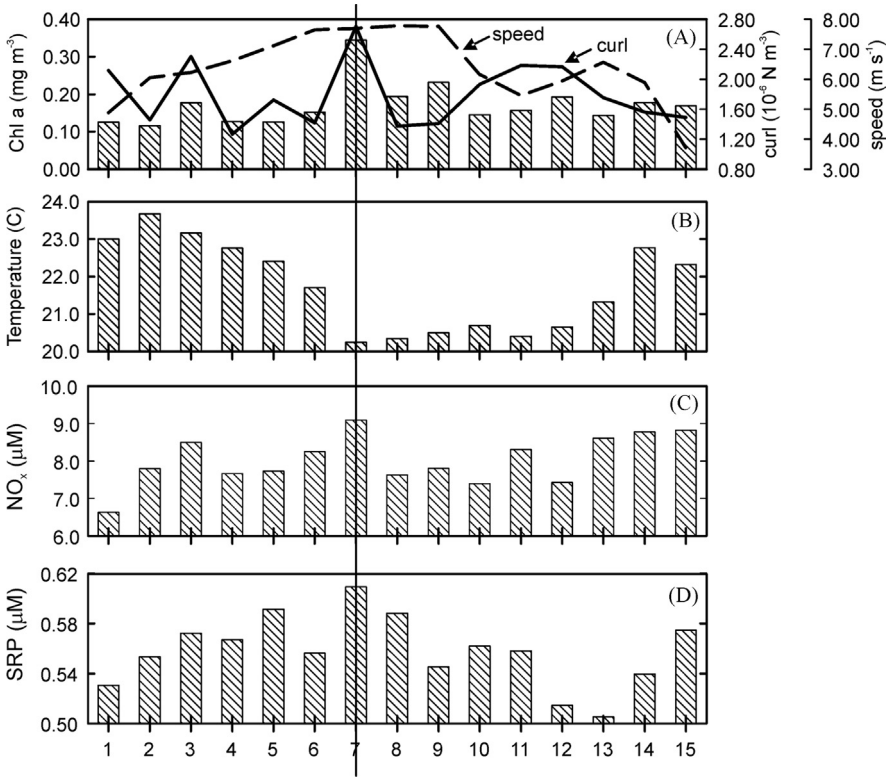

Fig. 5. The water column average (A) chlorophyll *a*, (B) water temperature and (C) nutrients (NO_x and SRP) across all sampling stations. Variations in wind-stress curl and wind speed are also plotted in panel (A) among all the sampling stations.

A Pearson Correlation analysis was carried out to evaluate the relationships between chlorophyll *a* concentration and wind parameters (wind-stress curl and wind speed) in the bloom region in late May. The correlation coefficient greater than 0.5 ($r > 0.5$) indicates high correlation between two parameters, whereas $r < 0.5$ presents weak correlation (P value is at the 0.01 level (2-tailed)). The results showed that chlorophyll *a* concentration and wind-stress curl were significantly correlated with each other ($r = 0.74$). The chlorophyll *a* concentration and wind speed had weak correlation ($r = 0.29$) (Fig. 7).

Fig. 8 illustrates the spatial distributions of chlorophyll *a*, *nLw* (443) and *nLw* (555) in late May. The pattern of low *nLw* (443) (Fig. 8, middle panel) was the same as the chlorophyll *a* pattern (Fig. 8, left panel). The *nLw* (555) distributions were uniform near 0 mW cm^{-2} μM^{-1} sr^{-1} in the phytoplankton region and nearby area (Fig. 4, right panel).

4. Discussion

4.1. Wind-stress curl induced variations of biological, chemical properties

This study has presented a description of the biological and chemical conditions of the ocean surface and at depth off the eastern Vietnam coast during the spring intermonsoon of 2010. The study area is offshore, and in these waters the surface chlorophyll *a* concentration is limited by nutrient availability rather than solar radiation, thus phytoplankton growth is largely restricted by nutrients (Tang et al., 2004a). The surface chlorophyll *a* concentration at Station 7 was about twice that at the other sampling locations. The high chlorophyll was associated with low nutrients (NO_x and SRP), and high dissolved oxygen at the surface layer. This was possibly due to phytoplankton growth consuming large amounts of nutrients and the photosynthetic release of oxygen (Miller, 2004). The nutrient profiles (NO_x and SRP) indicated that nutrients were low at shallow depths at Station 7, but here, nutrients levels in deep water were higher than that at other stations. Taking together the observations of phytoplankton growth-depleting nutrients, adequate nutrients being supplied from the deep layer at Station 7, and the relatively low dissolved oxygen and pH in the deep water, the results strongly suggest that deep sea water was being transported upwards in this region.

The subsurface chlorophyll maximum is a common feature in the open sea (Cullen, 1982). The subsurface chlorophyll maximum in the SCS varies from 50 m to 100 m with values between 0.1 mg m^{-3} to 0.6 mg m^{-3} in the SCS (Chen et al., 1989). The permanent subsurface chlorophyll maximum of SCS averages about 75 m depth at the bottom of euphotic zone (Chen et al., 1989). The present study indicated that the subsurface chlorophyll *a* concentration at Station 7 was three times as high as at other stations (Fig. 4A). The subsurface chlorophyll maximum was enhanced and uplifted to 50 m depth in this region (Fig. 4B). Most vertical variations of chlorophyll *a* in the sea can be attributed to the interactions between physical and biological processes (McClain et al., 1996). An enhanced subsurface chlorophyll maximum occurs episodically when physical processes increase the transfer of nutrients into the euphotic zone (McGillicuddy et al., 1998; Ning et al., 2004). This study area was located off the coast of Vietnam and light is not a limiting factor for the phytoplankton growth in this area (Tang et al., 2004b). Thus, phytoplankton grow rapidly in the euphotic zone wherever nutrients are sufficient (Wang et al., 2010). The subsurface chlorophyll maximum of the SCS is regulated by wind and the subsurface chlorophyll maximum with enhanced chlorophyll *a* often appears in the upwelling regions (Liu et al., 2002). Rarely have studies been focused on biological and physical

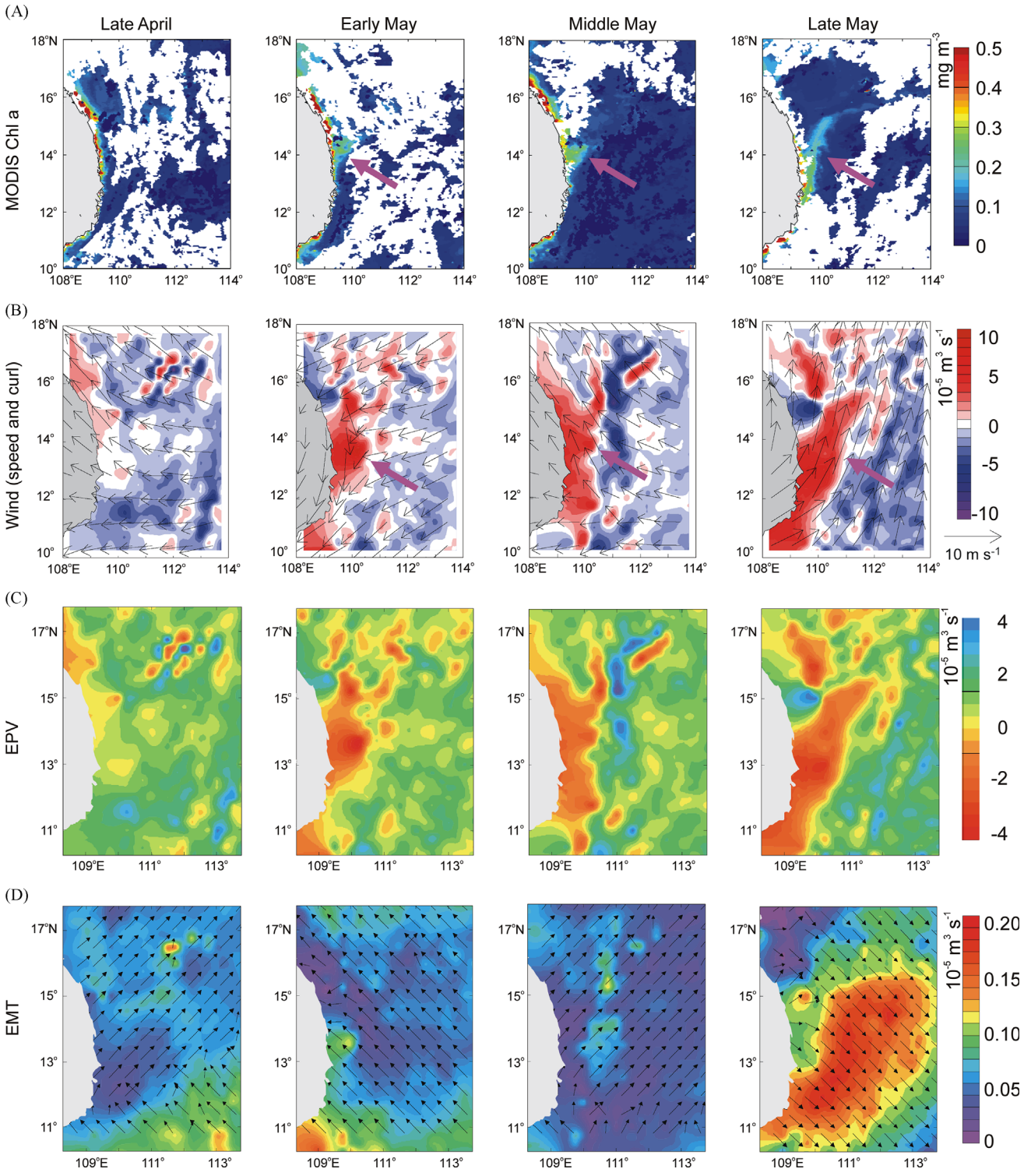

Fig. 6. (A) The spatial distribution of 8-day averaged MODIS Chl *a* concentrations (B) ASCAT wind speed with the contours of wind-stress curl; (C) Ekman pumping velocity; and (D) Ekman mass transport calculated from ASCAT wind data in late April (4/19–4/26), early May (4/27–5/4), mid-May (5/5–5/13), and late May (5/30–6/6), 2010. Bold arrows in (A) indicate the phytoplankton bloom region and in (B) the wind stress-curl region.

processes during the intermonsoon off the coastal Vietnam. In the following analysis, we mainly concentrated on the role of wind in phytoplankton growth and distribution.

The upper water column structure is affected by both atmosphere and internal oceanographic processes (Garrett, 1996). Wind-stress curl indicates variation in the wind, and depends on the spatial variations of winds rather than its magnitude and results in local divergences (Chereskin and Price, 2001). The changing trend of water column average chlorophyll *a* was the same as the wind-stress curl rather than wind speed. Rykaczewski and Checkley (2008) demonstrated that for long-term observations the chlorophyll *a* concentrations, as well as other seawater properties, are related positively with wind-stress curl in the upper ocean.

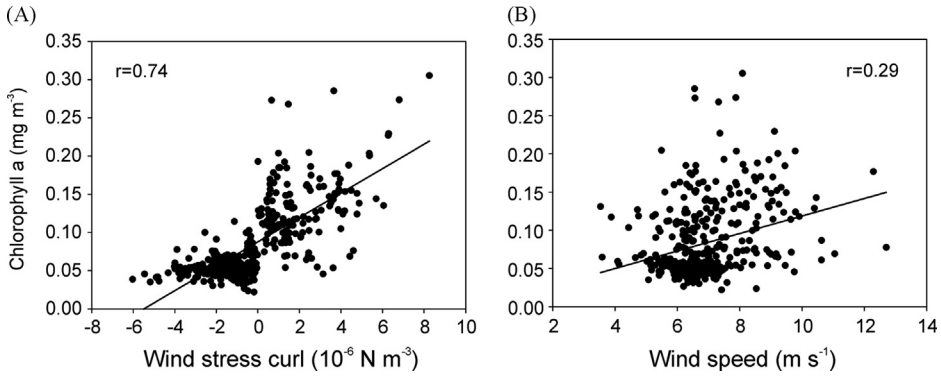

Fig. 7. Correlation between (A) MODIS chlorophyll *a* concentration and ASCAT-derived wind-stress curl and (B) MODIS chlorophyll *a* concentration and ASCAT-derived wind speed.

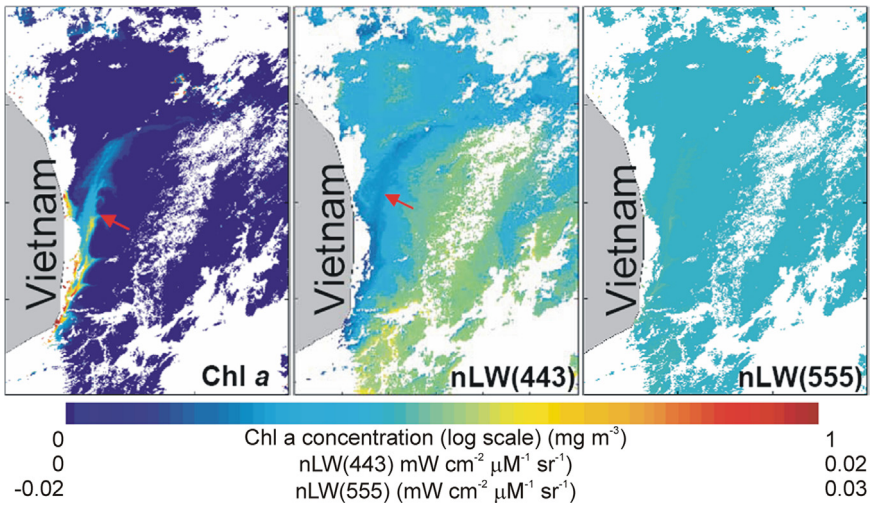

Fig. 8. Distributions of chlorophyll *a* concentrations (left panel), *nLw* (443) (middle panel), and *nLw* (555) (right panel). Data were derived from MODIS ocean color products for 30 May 2010.

4.2. *Wind-stress curl and the spatial distributions of phytoplankton*

Wind-stress curl can play a significant role in inducing high biological productivity zone with the consequential effects on marine ecology. For example, wind-stress curl gives rise to the spring bloom in the coastal Gulf of Alaska (Fiechter and Moore, 2009), and also contributes to the winter phytoplankton blooms in Luzon Strait (Peñaflor et al., 2007). Abbott and Barksdale (1991) show that wind-stress curl forces the variability of filaments and enhances the phytoplankton pigment patchiness in the California Current. During the spring intermonsoon 2010 in the South China Sea, the variation in phytoplankton patchiness was similar to the patterns of wind-stress curl, and a high chlorophyll *a* region was observed in an area of positive wind stress curl. Two types of upwelling are induced by different sea water movements: Ekman mass transport and Ekman pumping. Alongshore wind stress through Ekman mass transport results in costal upwelling with high vertical velocity. Ekman pumping and wind-stress curl result in curl-driven upwelling with a low vertical velocity (Rykaczewki et al., 2008). This study has demonstrated that upwelling during the spring intermonsoon was induced by wind-stress curl driving Ekman pumping, and not the coastal upwelling attributed to Ekman mass transport. The Ekman pumping (Fig. 3C) and Ekman mass transport (Fig. 3D) were exhibited with distinct patterns during spring intermonsoon 2010. If this is compared with the chlorophyll *a* distributions (Fig. 3A) during the same period, the results indicate that the spatial distribution pattern of negative Ekman pumping was similar to the phytoplankton bloom region, and the high chlorophyll *a* was confined to the high negative Ekman pumping area. Although the average Ekman pumping velocity was only ca. 10^{-5} m s^{-1}, the consistent vertical movement can transport nutrients from the ocean interior to the upper layer (Chereskin and Price, 2001).

Sampling was carried out during the formation of a phytoplankton bloom in the region of positive wind-stress curl and negative Ekman pumping (Station 7; Figs. 1B; 6). The nutrient flux appeared to be adequate to sustain high phytoplankton biomass in the euphotic zone, and then the subsurface chlorophyll maximum was enhanced and uplifted through upwelling in the curl-driven upwelling region. The high Ekman pumping induced by wind-stress curl may strengthen local vertical mixing of sea water. Furthermore, cold water with adequate nutrients was pumped into the upper layer with increasing wind-stress curl. The vertical movement of sea water in the upper layer supplies nutrients from deep waters for the phytoplankton growth in the euphotic zone (Ueyama and Monger, 2005).

Statistical analysis further demonstrated a high correlation between chlorophyll *a* concentration and wind-stress curl ($r > 0.5$) and weak correlation between chlorophyll *a* concentration and wind speed ($r < 0.5$) (Fig. 7). This conclusion was highly consistent with the results of Pearson Correlation analysis by Peñaflor et al. (2007) in the Luzon Strait. Their results showed that a high frequency of positive curl coincided with the timing of bloom occurrence and there was significant correlation between the two. In other researches, Fiechter and Moore (2009). using a modeling approach, also verified that the interannual variability

in phytoplankton blooms is related to the interannual variability of wind-stress curl in the northwestern coastal Gulf of Alaska (Fiechter and Moore, 2009).

The formation of the phytoplankton bloom was largely unaffected by suspended sediment and influx in the coastal waters. The low *nLw* (443) of phytoplankton absorption and the high chlorophyll *a* concentration had the same pattern, indicating ocean color images could illustrate the phytoplankton distributions more accurately (Shi and Wang, 2007). The *nLw* (555) reflected the influence of discharges from the coast (Zheng and Tang, 2007). The uniform *nLw* (555) in the bloom and nearby region further confirmed that the nutrient source was not from the coastal water. In addition, the observed spring phytoplankton patchiness off the eastern coast of Vietnam was not an isolated incident in 2010. We studied the ocean color data over the past ten years and have found that the spring phytoplankton patchiness can be detected in April or May nearly every year (data not shown).

4.3. Differences between phytoplankton blooms in summer and spring

We compared the conceptual mechanisms of phytoplankton blooms between spring and summer (Fig. 9). During the spring intermonsoon, the phytoplankton bloom appears off the eastern Vietnam coast and extends into the western SCS. Chaotic winds with varied wind directions could not induce the prolonged coastal upwelling, but wind-stress curl gives rise to upwelling via Ekman pumping. Wind-stress curl plays an important role in the distribution of chlorophyll *a* and enhances the pigment patterns (Abbott and Barksdale, 1991). Deep cold water with low dissolved oxygen can be a source of nutrients that sustains the phytoplankton growth through this kind of upwelling (Tang et al., 1999). Our study has demonstrated that wind-stress curl affected not only the spatial distribution pattern of phytoplankton bloom, but also its vertical structure off the eastern Vietnam coast during the spring intermonsoon. The connection between wind-stress curl and phytoplankton bloom is curl-driven upwelling through Ekman pumping (Huyer et al., 2005), and as a consequence, phytoplankton patchiness is observed in the region of positive Ekman pumping.

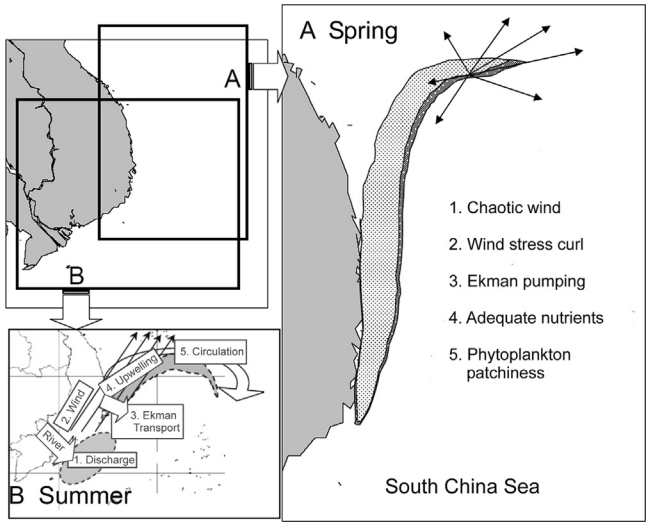

Fig. 9. Conceptual models representing the mechanisms involved in (A) the spring phytoplankton bloom off the eastern Vietnam coast in the South China Sea and (B) summer phytoplankton blooms off the southeastern Vietnam coast in the South China Sea.
Modified from Tang et al. (2004a, 2004b).

Wind direction can however play an important role in coastal upwelling (Tang et al., 2005). In summer, the persistent alongshore southwest monsoon forces an offshore Ekman transport inducing coastal upwelling (Kuo et al., 2000; Tang et al., 2004a, 2004b). Coastal upwelling is normally attributed to wind which prevails along the coastline for a period. This coastal upwelling is largely due to wind stress rather than wind-stress curl (Hwang and Chen, 2000), and delivers nutrients to surface waters to support phytoplankton growth (Tang et al., 2004a). Subsequently, the phytoplankton distribution forms a coastal filament from an anticyclonic circulation (Tang et al., 2004b, 2005).

5. Conclusions

Upwelling induced by positive wind-stress curl gave rise to the phytoplankton patchiness during the spring intermonsoon off the eastern Vietnam coast in the SCS. Curl-driven upwelling pumped nutrients from the deep sea into the euphotic zone to fuel the spring phytoplankton bloom, regardless of how the wind directions varied during the spring intermonsoon period. The enhanced and uplifted subsurface chlorophyll maximum within the euphotic zone was associated with intense Ekman pumping. In addition, the distributions of phytoplankton patchiness were restricted by wind-stress curl. The present study demonstrated that wind-stress curl played a significant role in regulating the vertical structure of biological and chemical properties and the spatial distribution of phytoplankton biomass during spring intermonsoon in the sea.

This study provides scientific evidence that biological and physical interactions during the intermonsoon period merit investigation off the Vietnam coast in the SCS. This work distinguishes between the mechanisms of phytoplankton bloom formation in different seasons.

Acknowledgments

This study was supported by the following research projects awarded to Professor DanLing Tang: (1) National Natural Sciences Foundation of China (31061160190, 40976091); (2) Natural Sciences Foundation of Guangdong China (8351030101000002, 2010B031900041); (3) Group program (2013) of State Key Laboratory of Tropical Oceanography, South China Sea Institute of Oceanology, Chinese Academy of Sciences (LOT-ZZ-1301); and (4) NSFC-RFBR Project (41211120181) awarded to DL Tang and D. Pozdnyakov.

References

Abbott, M.R., Barksdale, B., 1991. Phytoplankton pigment patterns and wind forcing off central California. J. Geophys. Res. 96 (C8), 14649–14667, http://dx.doi.org/10.1029/91JC01207.

Botsford, L.W., Lawrence, C.A., Dever, E.P., Hastings, A., Largier, J., 2006. Effects of variable winds on biological productivity on continental shelves in coastal upwelling systems. Deep Sea Res. Part II 53 (25–26), 3116–3140.

Cloern, J.E., 1996. Phytoplankton bloom dynamics in coastal ecosystems: a review with some general lessons from sustained investigation of San Francisco Bay, California. Rev. Geophys. 34 (2), 127–168.

Corrigan, C.E., Ramanathan, V., Schauer, J.J., 2006. Impact of monsoon transitions on the physical and optical properties of aerosols. J. Geophys. Res. 111, D18208, http://dx.doi.org/10.1029/2005JD006370.

Chereskin, T.K, Price, J.F., 2001. Ekman transport and pumping. In: Steele, J.H., et al. (Eds.), Encyclopedia of Ocean Sciences, Eds. Academic Press, London, pp. 809–815.

Cullen, J.J., 1982. The deep chlorophyll maximum: comparing vertical profiles of chlorophyll a. Can. J. Fish. Aquat. Sci. 39, 791–803.

Chen, X.Q., Chen, Q.H., Zhuang, L.Z., 1989. The relationships among the Chlorophyll a distribution, photosynthesis and environmental factor in the center of South China Sea. Acta Oceanol. Sin. 3 (11), 349–355. (in Chinese).

Dippner, J.W., Nguyen, K.V., Hein, H., Ohde, T., Loick, N., 2007. Monsoon-induced upwelling off the Vietnamese coast. Ocean Dyn. 57 (1), 46–62.

Fiechter, J., Moore, A.M., 2009. Interannual spring bloom variability and Ekman pumping in the coastal Gulf of Alaska. J. Geophys. Res. – Oceans 114.
Garrett, C., 1996. Processes in the surface mixed layer of the ocean. Dyn. Atmos. Oceans 23, 19–34.
Huyer, A., Fleischbein, J.H., Keister, J., Kosro, P.M., Perlin, N., Smith, R.L., Wheeler, P. A., 2005. Two coastal upwelling domains in the northern California Current system. J. Mar. Res. 63 (5), 901–929.
Hwang, C., Chen, S.-A., 2000. Circulations and eddies over the South China Sea derived from TOPEX/Poseidon altimetry. J. Geophys. Res. 105 (C10), 23943–23965, http://dx.doi.org/10.1029/2000JC900092.
Hai, D.N., Lam, N.N., Dippner, J.W., 2010. Development of *Phaeocystis globosa* blooms in the upwelling waters of the South Central coast of Viet Nam. J. Mar. Syst. 83 (3–4), 253–261.
Kuo, N.J., Zheng, Q.N., Ho, C.R., 2000. Satellite observation of upwelling along the western coast of the South China Sea. Remote Sensing Environ. 74 (3), 463–470.
Lin, I.-I., Lien, C.-C., Wu, C.-R., Wong, G.T.F., Huang, C.-W., Chiang, T.-L., 2010. Enhanced primary production in the oligotrophic South China Sea by eddy injection in spring. Geophys. Res. Lett. 37, L16602, http://dx.doi.org/10.1029/2010GL043872.
Liu, K.K., Chao, S.Y., Shaw, P.T., Gong, G.C., Chen, C.C., Tang, T.Y., 2002. Monsoon-forced chlorophyll distribution and primary production in the South China Sea: observations and a numerical study. Deep-Sea Res. Part I 49 (8), 1387–1412.
McGillicuddy, D.J., Robinson, A.R., Siegel, D.A., Jannasch, H.W., Johnson, R., Dickeys, T., McNeil, J., Michaels, A.F., Knap, A.H., 1998. Influence of mesoscale eddies on new production in the Sargasso Sea. Nature 394 (6690), 263–266.
McGillicuddy, D.J., Anderson, L.A., Doney, S.C., Maltrud, M.E., 2003. Eddy-driven sources and sinks of nutrients in the upper ocean: results from a 0.1 degrees resolution model of the North Atlantic. Global Biogeochem. Cycles 17 (2), 1035, http://dx.doi.org/10.1029/2002GB001987.
Miller, C.B., 2004. Biological Oceanography. Wiley Blackwell Publishing Malden, MA, pp. 9–15.
McClain, C.R., Arrigo, K., Tai, K.S., Turk, D., 1996. Observations and simulations of physical and biological processes at ocean weather station P, 1951–1980. J. Geophys. Res. 101, 3697–3713.
Ning, X., Chai, F., Xue, H., Cai, Y., Liu, C., Shi, J., 2004. Physical–biological oceanographic coupling influencing phytoplankton and primary production in the South China Sea. J. Geophys. Res. 109, 1–20.
Oudot, C., Gerard, R., Morin, P., Gningue, I., 1988. Precise shipboard determination of dissolved-oxygen (Winkler Procedure) for productivity studies with a commercial system. Limnol. Oceanogr. 33 (1), 146–150.
Pomeroy, L.R., Sheldon, J.E., Sheldon, W.M., 1994. Changes in bacterial numbers and leucine assimilation during estimations of microbial respiratory rates in seawater by the precision Winkler method. Appl. Environ. Microbiol. 60 (1), 328–332.
Peñaflor, E.L., Villanoy, C.L., Liu, C.-T., David, L.T., 2007. Detection of monsoonal phytoplankton blooms in Luzon Strait with MODIS data. Remote Sensing Environ. 109 (4), 443–450.
Rykaczewski, R.R., Checkley Jr., D.M., 2008. Influence of ocean winds on the pelagic ecosystem in upwelling regions. Proc. Natl. Acad. Sci. USA 105 (6), 1965–1970.
Shi, W., Wang, M., 2007. Observations of a Hurricane Katrina-induced phytoplankton bloom in the Gulf of Mexico. Geophys. Res. Lett. 34, L11607, http://dx.doi.org/10.1029/2007GL029724.
Strickland, J.D.H., Parsons, T.R., 1972. A Practical Handbook of Seawater Analysis, 2nd edn. Fisheries Research Board of Canada, Canada p. 310.
Stewart, R.H., 2008. Introduction to Physical Oceanography. Texas A & M University, Texas, pp. 133–147.
Tang, D.L., Kawamura, H., Shi, P., Takahashi, W., Shimada, T., Sakaida, F., Isoguchi, O., 2005. Seasonal phytoplankton blooms associated with monsoonal influences and coastal environments in the sea areas either side of the Indochina Peninsula. J. Geophys. Res. – Biogeosci. 111, G01010, http://dx.doi.org/10.1029/2005JG000050.
Tang, D.L., Kester, D.R., Ni, I.H., Kawamura, H., Hong, H., 2002. Upwelling in the Taiwan Strait during the summer monsoon detected by satellite and shipboard measurements. Remote Sensing Environ. 83 (3), 457–471.
Tang, D.L., Ni, I.H., Kester, D.R., Muller-Karger, F.E., 1999. Remote sensing observations of winter phytoplankton blooms southwest of the Luzon Strait in the South China Sea. Mar. Ecol. – Prog. Ser. 191, 43–51.
Tang, D.L., Kawamura, H., Dien, T.V., Lee, M.A., 2004a. Offshore phytoplankton biomass increase and its oceanographic causes in the South China Sea. Mar. Ecol. Prog. Ser. 268, 31–41.
Tang, D.L., Kawamura, H., Doan-Nhu, H., Takahashi, W., 2004b. Remote sensing oceanography of a harmful algal bloom off the coast of southeastern Vietnam. J. Geophys. Res. – Oceans 109.
Ueyama, R., Monger, B.C., 2005. Wind-induced modulation of seasonal phytoplankton blooms in the North Atlantic derived from satellite observations. Limnol. Oceanogr. 50 (6), 1820–1829.
Voss, M., Bombar, D., Loick, N., Dippner, J.W., 2006. Riverine influence on nitrogen fixation in the upwelling region off Vietnam, South China Sea. Geophys. Res. Lett. 33, L07604, http://dx.doi.org/10.1029/2005GL025569.
Wang, J.J., Tang, D.L., Su, Y., 2010. Winter phytoplankton bloom induced by subsurface upwelling and mixed layer entrainment southwest of Luzon Strait. J. Mar. Syst. 83 (3–4), 141–149.
Xie, S.-P., Xie, Q., Wang, D., Liu, W.T., 2003. Summer upwelling in the South China Sea and its role in regional climate variations. J. Geophys. Res. 108 (C8), 3261, http://dx.doi.org/10.1029/2003JC001867.
Zheng, G.M., Tang, D.L., 2007. Offshore and nearshore chlorophyll increases induced by typhoon winds and subsequent terrestrial rainwater runoff. Mar. Ecol. Prog. Ser. 333, 61–74.